DOI 10.1007/s11041-018-0253-y
Metal Science and Heat Treatment, Vol. 60, Nos. 3 – 4, July, 2018 (Russian Original Nos. 3 – 4, March – April, 2018)

UDC 669.017.16

SPECIAL FEATURES OF PRECIPITATION OF ε-Cu PHASE IN CAST IRONS ALLOYED WITH COPPER AND ALUMINUM

A. A. Bataev,[1] N. V. Stepanova,[1] I. A. Bataev,[1] Y. Kang,[2] and A. A. Razumakov[1]

Translated from *Metallovedenie i Termicheskaya Obrabotka Metallov*, No. 3, pp. 18 – 25, March, 2018.

Special features of precipitation of ε-Cu phase in cast irons alloyed with copper and aluminum are studied. The FactSage software is used to amend the Fe – Cu – C phase diagram. The diagram is used to analyze the structure of the metals. The shape of the particles and the places of their localization in the volume of the alloys are determined by x-ray diffraction analysis. The causes of the hardening action of copper in the irons are assessed.

Key words: cast iron, structure, ε-Cu, hardness, Fe – Cu – C phase diagram.

INTRODUCTION

Copper-alloyed cast irons are sometimes used as materials for tribotechnical applications and an alternative to costly bronzes [1, 2]. Economically, it is the most expedient to replace bronze with cast iron in the production of large-size heavily loaded sliding friction units. The operating conditions of such units involve application of high unit loads. Consequently, the materials for such units should combine high strength and tribotechnical properties. One of the most important structural factors determining the level of these properties in copper-alloyed alloys is connected with the volume fraction, sizes, geometry and distribution of the copper-containing precipitates. The role of this factor is especially important in Fe – Cu alloys, because the solubility of copper in iron at room temperature is negligibly low [3]. Therefore, copper precipitates during cooling of the alloys almost entirely and is contained in the metal in the form of isolated microvolumes of an ε-Cu phase represented by a solid solution of iron in the fcc lattice of copper [4].

Iron-carbon alloys containing precipitates of ε-Cu have been studied in many works [5 – 15]. Most of them are devoted to analysis of the effect of copper on the structure and properties of steels. Copper-alloyed cast irons have attracted much less attention. The effect of copper on graphitization and tribotechnical properties of cast irons is described in [2]. Optical metallography and transmission electron microscopy used to study their structure have shown a variety of shapes and sizes of particles of ε-Cu. The sizes of the precipitates of ε-Cu in the same alloy may differ substantially. It is obvious that the effect of these particles on the combination of the strength and tribotechnical properties of the metal should differ too. These aspects are not described systematically in the relevant literature. The mechanisms of formation of ε-Cu precipitates in copper-alloyed cast irons have not been described in detail.

The aim of the present work was to study the special features of precipitation of the ε-Cu phase in cast irons alloyed with copper and aluminum.

METHODS OF STUDY

We studied four sand-loam-cast castings of iron alloyed with copper (from 0.08 to 14.7% Cu)[3] and aluminum (0.9% Al). The castings were shaped as cylinders 500 mm high and 90 mm in diameter. The blend was melted in a crucible induction furnace. In all the cases the metal was cast at 1350°C. The elemental composition of the cast metal was determined with the help of an ARL 3460 optical emission spectrometer. The results of the analysis of the materials obtained are presented in the Table. The content of aluminum was the same in all the castings (0.9%). This element was introduced to raise the uniformity of the distribution of ε-Cu

[1] Novosibirsk State Technical University, Novosibirsk, Russia (e-mail: stepanova@adm.nstu.ru).
[2] University of Science and Technologies, Institute of Ferrous Metallurgy, Pohang, Republic of Korea.

[3] Here and below in the paper the content of the elements is given in mass percent.

TABLE 1. Chemical Compositions of Cast Irons

Alloy	Content of elements, wt.%								
	C	Mn	Si	P	S	Ni	Cr	Cu	Al
SCh0.1Cu	2.90	0.51	0.23	0.01	0.01	0.04	0.04	0.08	0.9
SCh3.3Cu	2.91	0.50	0.24	0.01	0.01	0.04	0.03	3.27	0.9
SCh6.6Cu	2.89	0.51	0.22	0.01	0.01	0.03	0.04	6.57	0.9
SCh14.7Cu	2.87	0.52	0.23	0.01	0.01	0.04	0.04	14.7	0.9

particles over the volume of the metal [4, 16]. The metallographic studies were conducted with the help of a Carl Zeiss Axio Observer Z1m microscope. The laps were prepared by a standard technique involving mechanical grinding and subsequent polishing. The structure of the alloys was uncovered by chemical etching of the laps with a 4% solution of nitric acid in ethyl alcohol. The structure of the alloys was studied under a Carl Zeiss EVO 50 XVP scanning electron microscope and a FEI Tecnai G2 20 TWIN transmission electron microscope.

The hardness of the materials was determined by the Brinell method at a load of 30 kN on the indenter. To estimate the properties of the structural components in the metal we measured the Vickers hardness using a Wolpert Group 402MVD device at a load of 1 N on the diamond indenter.

RESULTS AND DISCUSSION

Fe – Cu – C Phase Diagram

A circumstance that turns us to the problem is amendment of the Fe – Cu – C phase diagram, analysis of which should allow us to associate the features of nucleation of ε-Cu particles with the conditions of crystallization of the alloys. In addition, advanced analytical equipment, transmission electron microscopes in the first turn, allows us to detect some not yet described details of the structure of very fine particles of ε-Cu.

It is expedient to correlate the origin and the structural features of the components appearing in the analyzed alloys and their phase diagram. The main components of the alloys studied are iron, copper and carbon. Therefore, we turned to analyzing the Fe – Cu – C system. Recent literature gives only fragmentary data on the phase diagram of this three-component system. For example, the sections of the Fe – Cu – C diagram in [17 – 19] give data on alloys with a low carbon content or have been designed for a limited temperature range and are inapplicable for analysis of the succession of the phase transformations occurring under crystallization of copper-alloyed cast irons. In the present work, we used the results of the thermodynamic computations of Shubhank and Kang [18] obtained with the use of the FactSage software to design the isopleth section of the Fe – Cu – C phase diagram for 3% C and from 0 to 40% Cu. The results of the computations are presented in Fig. 1.

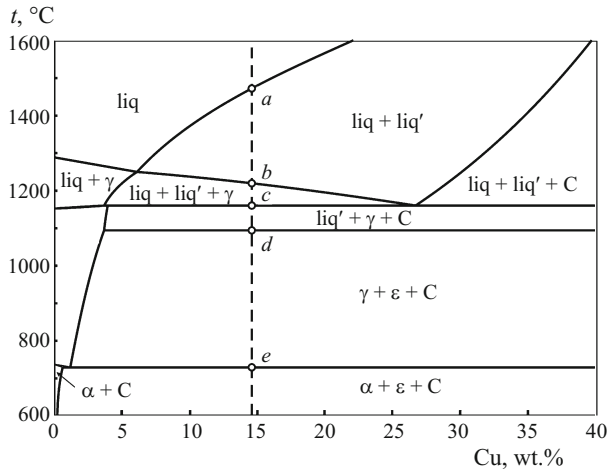

Fig. 1. Isopleth (polythermal) section of the Fe – Cu – C phase diagram matching the alloys with 3% C: liq and liq′) iron- and copper-enriched liquid, respectively; C) graphite; γ) iron-base fcc solid solution; α) iron-base bcc solid solution; ε) copper-base fcc solid solution.

The phase diagram obtained can be used to determine the succession of the structural transformations in copper-alloyed cast irons. Let us consider the changes occurring in the alloy containing 14.7% Cu and 3% C (the dashed line in Fig. 1) as an example. At the temperature above point *a* (about 1480°C) the alloy has a state of single-phase liquid. At 1480 – 1220°C (between points *a* and *b*) the liquid stratifies into copper-enriched and copper-depleted phases. With decrease in the temperature, the content of the copper-enriched phase increases. At point *b* hypoeutectic crystals of γ-iron start to precipitate in the copper-depleted liquid. When the temperature falls to point *c* (about 1155°C), the volume fraction of the austenite increases, and the content of the copper-depleted liquid decreases.

The temperature of about 1155°C corresponds to a eutectic transformation, which yields a mechanical mixture. The diagram presented in Fig. 1 stipulates formation of a eutectic consisting of austenite and graphite. The copper-enriched liquid does not participate in the eutectic reaction. When the temperature decreases still more, its content even increases due to retrograde melting and precipitation of copper from the austenite in the temperature range of 1155 – 1096°C

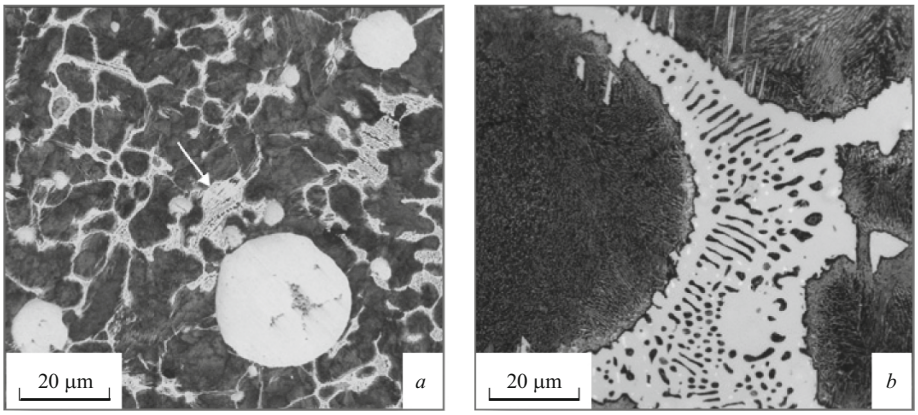

Fig. 2. Ledeburite colonies in the structure of SCh14.7Cu iron (marked with the arrows).

(point *d* in Fig. 1). At about 1096°C (point *d* in Fig. 1) the entire copper-enriched liquid present on the alloy crystallizes. Subsequent transformations develop in solid state. In the temperature range between points *d* and *e*, i.e., in the process of cooling to 730°C, the solubility of copper in the austenite decreases, and particles of ε-Cu precipitate in the volume of the metal. Upon attainment of point *e* (about 730°C), the system acquires a "α-Fe – ε-Cu – graphite" ternary eutectoid.

Subsequent cooling to room temperature is accompanied by additional precipitation of ε-Cu and graphite due to the gradual decrease in the solubility of carbon and copper in the ferrite. It should also be noted that the considerable change in the solubility of iron in copper upon decrease of the temperature should yield inclusions of α-Fe inside the particles of ε-Cu formed as a result of primary crystallization, and then inclusions of α-Fe under further cooling.

Metallographic and Electron Microscope Studies of Alloyed Cast Irons

It should be noted that the Fe – Cu – C diagram presented in Fig. 1 has been designed for the alloys in equilibrium condition. In accordance with it, carbon should precipitate during cooling of the metal in the form of stable phase, i.e., graphite. The results of the analysis of the structure of actual castings show that the phase transformations occurring in the stage of crystallization of the alloys are not equilibrium ones. A typical feature of such deviations is formation of a metastable cementite phase, which enters the colonies of pearlite and ledeburite, instead of graphite. When the copper content in the analyzed alloys is increased, the susceptibility to formation of cementite grows. These circumstances determine the most significant deviations of the structure of the obtained cast irons from the equilibrium Fe – Cu – C diagram.

Alloy SCh0.1Cu with minimum content of copper (0.08%) is gray iron based on ferrite and pearlite. The volume fraction of ferrite in it amounts to about 1%; the graphite has the form of plates about 100 μm long, and its amount is 7.8%. The interplate distance in the pearlite is 0.65 μm. Growth in the copper concentration affects all the structural components of the cast irons. Introduction of 3.27% Cu into the metal results in full removal of ferrite grains from the structure. The fineness of the plate pearlite in the metal increases with the copper content. In the iron containing 14.7% Cu, the interplate distance is reduced to 0.4 μm. One of the most probable causes of this change is connected with the change in the thermal conductivity of the alloy, which in its turn affects the rate of its crystallization [20]. The content of graphite decreases with growth of the copper content to 6.57%. This means that copper is an element promoting chilling of the iron. In alloy SCh14.7Cu graphite is virtually absent. Colonies of ledeburite are distributed uniformly over the volume of the casting (see Fig. 2*a*). The structure of the microvolumes of pearlite distributed inside cementite crystals reflects a cellular morphology typical for ledeburite colonies (Fig. 2*b*).

We concentrated in the structural studies on the special features of precipitation of microvolumes of ε-Cu. In the SCh0.1Cu and SCh3.3Cu alloys we detected no inclusions of ε-copper by the methods of optical microscopy. Single microvolumes about 1 – 2 μm in size were detected only when the copper content was raised to 6.57%.

The widest spectrum of ε-Cu inclusions was observed in the SCh14.7Cu alloy. The features of its structure are shown schematically in Fig. 3. The coarsest particles have an almost globular shape (Figs. 2*a* and 3*a*). This shape of the ε-Cu inclusions is a result of stratification of the melt in the temperature range between points *a* and *b* and formation of a two-phase emulsion (Fig. 1). The fraction of the analyzed particles in the volume of the iron obtained amounts to 3.35%. The austenite crystals formed under the cooling of the material to the solidus line do not virtually change the globular form of the copper-containing drops. The size distribution of the particles is presented in Fig. 4. The diameter of the coarsest inclusions reaches about 250 μm. The peak of the distribution of globular inclusions of ε-Cu corresponds to the sizes of 20 – 30 μm.

In the temperature range of 1155 – 1096°C corresponding to points b and c in Fig. 1, the main structural components of alloy SCh14.7Cu are austenite, ledeburite and a liq-

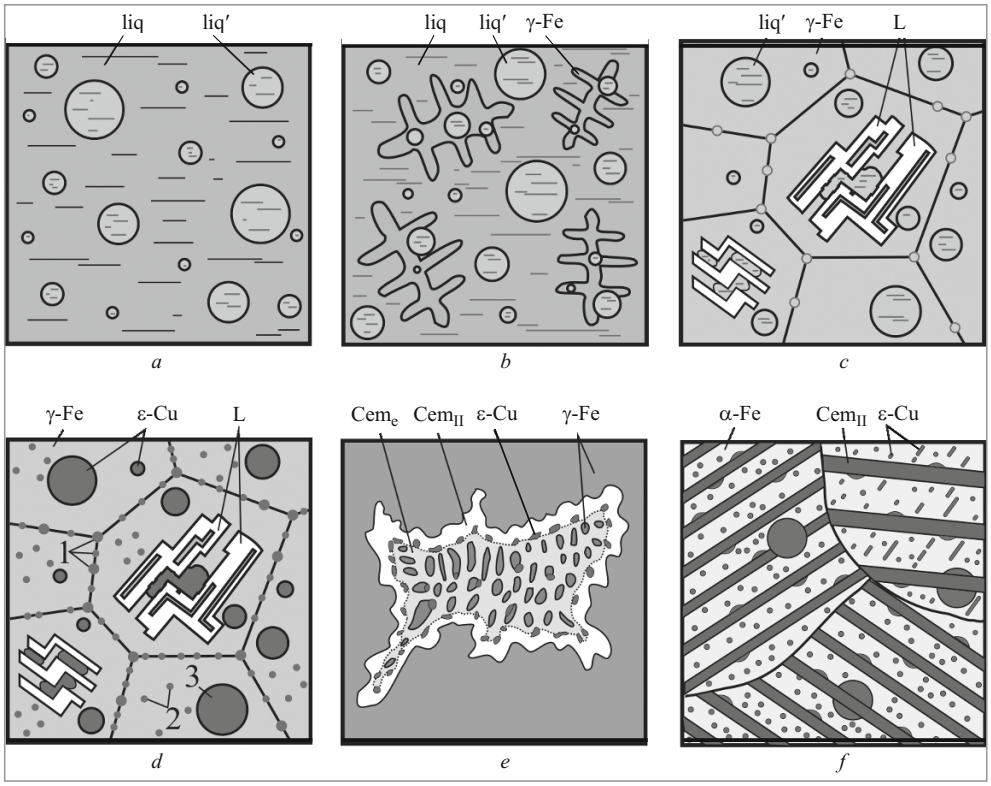

Fig. 3. Diagrams of precipitation of copper-enriched phase in cast iron containing 2.9% C and 14.7 Cu: *a*, *b*, *c*, *d*) between points *a* and *b*, *b* and *c*, *c* and *d*, and *d* and *e* of the scheme of Fig. 1, respectively; *e*) special feature of formation of ε-Cu particles in the cementite; *f*) diagram of the structure formed below point *e* in the scheme; L) ledeburite; Cem_e and Cem_{II}) crystals of eutectic and secondary cementite.

uid solution of iron in copper. The copper-containing inclusions located within the ledeburite colonies have an irregular shape (see Fig. 5*a*). There are many particles of ε-Cu between the Fe3C crystals. The mechanism of formation of such microvolumes is explainable by contragrowth of cementite crystals. If they are separated by a drop of a copper-base liquid solution, the growing cementite crystals deform it mechanically (Fig. 3*d*). For this reason, the absolute majority of the ε-Cu inclusions located within the ledeburite colonies do not have a globular shape.

Cooling of the alloy in the whole of the range of existence of the α-Fe phase should be accompanied in accordance with the phase diagram by precipitation of microvolumes of a copper-based solution from the austenite. At the temperatures above 1096°C the solution precipitates in a liquid-phase state. In the temperature range between points *d* and *e* (1096 – 730°C) the particles of ε-Cu precipitate in a solid-phase state (Fig. 1). The places of preferred precipitation of ε-Cu are boundaries of the austenite grains. In the structure of SCh14.7Cu we detected regions of boundaries decorated with numerous ε-Cu particles about 1 – 5 μm in size (Fig. 6*a* and particles *1* in Fig. 3*d*). It is obvious that the whole of the copper that should precipitate from phase α-Fe in accordance with the phase diagram cannot be concentrated in inclusions over austenite boundaries when the temperature of the alloy decreases. The volume of the retained copper, which exceeds its limiting solubility in the austenite, precipitates inside the austenite grains in the form of ε-Cu particles with an almost globular shape. Numerous inclusions of this kind are well observable against the background of colonies

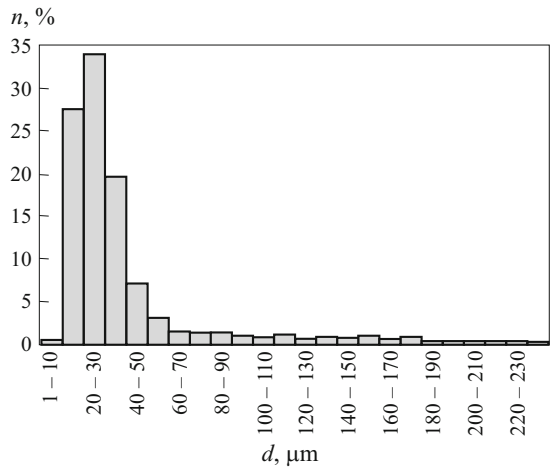

Fig. 4. Size (diameter) distribution of ε-Cu particles in cast iron SCh14.7Cu (*n* is the number of cases).

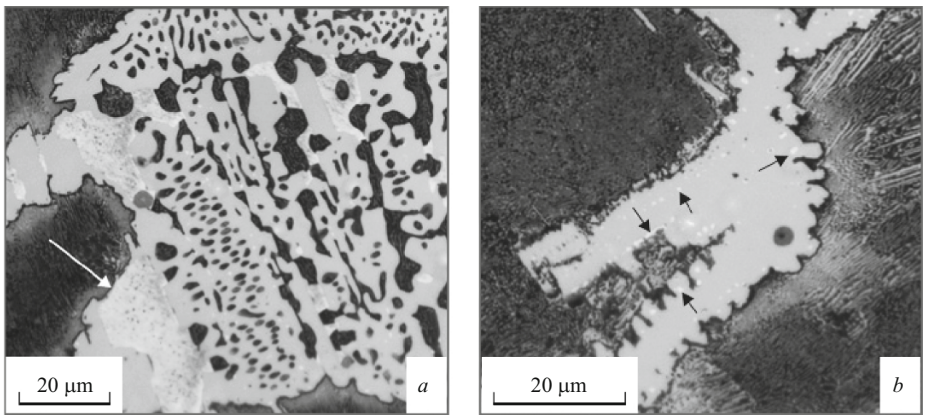

Fig. 5. Inclusions of ε-Cu (marked with the allows) in a ledeburite colony (*a*) and inside cementite crystals (*b*) in cast iron SCh14.7Cu.

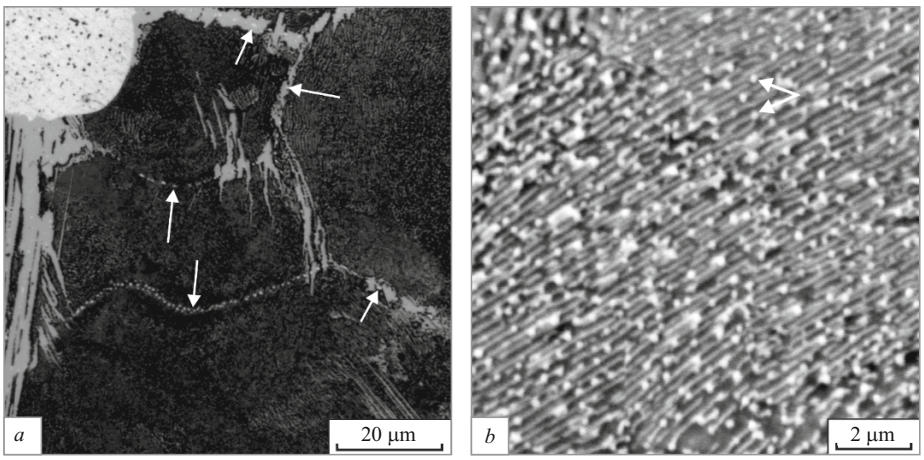

Fig. 6. Particles of ε-Cu (marked with the arrows) precipitated over boundaries (*a*) and inside (*b*) austenite grains in cast iron SCh14.7Cu.

of plate pearlite in the form of light points (Figs. 6*b* and particles *2* in Fig. 3*d*). The size of these precipitates is about 200 nm, which is about an order of magnitude smaller than the size of the grain-boundary particles of ε-Cu (particles *1* in Fig. 3*d*) and 2 – 3 orders of magnitude smaller that the ε-Cu particles precipitated form the two-phase emulsion (particles of type *3* in Fig. 3*d*).

The metallographic study has shown the presence of one more type of ε-Cu particles within cementite crystals (see Fig. 5*b*). Their characteristic feature is dominant precipitation in the form of a necklace in the near-boundary layer inside large carbides. A scheme of the possible mechanism of formation of a heterophase structure with particles of ε-Cu decorating the external layer of carbide precipitates is presented in Fig. 3*e*. It shows that growth of a crystal of eutectic cementite is accompanied by squeezing of copper and its preferred precipitation in the form of microvolumes of ε-Cu phase over the contour of a carbide. In subsequent growth of secondary cementite on the eutectic carbides these particles are surrounded with cementite on all sides. As a rule, such ε-Cu particles have an irregular shape and their size amounts to about 1 – 2 μm.

The finest particles of ε-Cu with a size of 5 – 30 nm precipitate in ferrite spaces of the plate pearlite. For this reason, they can be detected reliably only by the method of transmission electron microscopy (Fig. 7). Formation of such a fine dispersed pattern is explainable by the extremely low solubility of copper in the α-Fe at room temperature. The limited mobility of copper atoms in the ferrite is a factor retarding the growth of ε-Cu particles.

Figure 7*a* presents the fine structure of a colony of plate ferrite in cast iron of type SCh14.7Cu. We can observe two types of compact globular precipitates of ε-Cu, the size of which differs by an order of magnitude, within ferrite spaces. The size of the coarsest ε-Cu particles (Fig. 7*a*) is commensurable to the thickness of the ferrite spaces in the colonies of plate pearlite. Analysis the diffraction data and of the Fe – Cu – C phase diagram allows us to infer that these particles of ε-Cu have precipitated from the austenite prior to the start of the pearlitic transformation, i.e., the colony of plate pearlite has appeared within the two-phase (γ-Fe + ε-Cu) mixture rather than in the homogeneous austenite. During the growth of the pearlite colony, the particles of ε-Cu arranged randomly inside the austenite grains are built into cementite plates. The susceptibility of the cementite to precipitation of particles of ε-Cu explains convincingly the mentioned feature of this kind of heterophase structure. Comparing the analyzed particles to the earlier presented schemes of structure

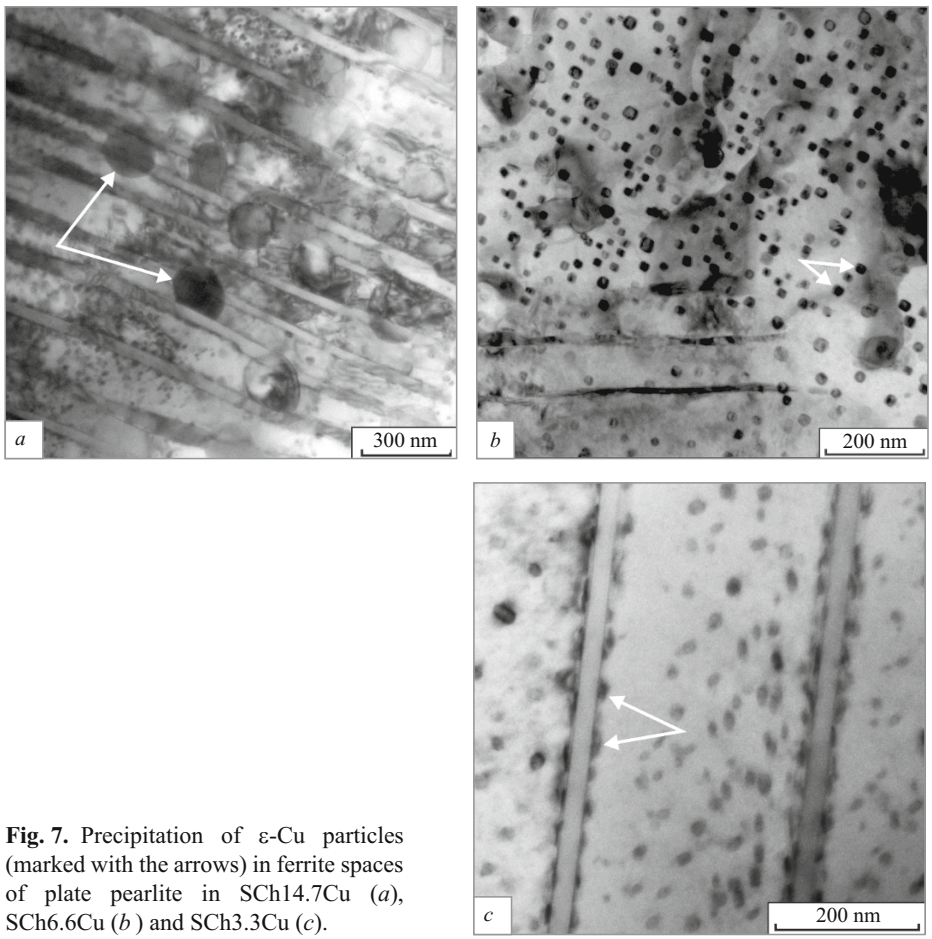

Fig. 7. Precipitation of ε-Cu particles (marked with the arrows) in ferrite spaces of plate pearlite in SCh14.7Cu (*a*), SCh6.6Cu (*b*) and SCh3.3Cu (*c*).

formation in cast iron, we may state that the coarser precipitates of ε-Cu detectable in Fig. 7*a* correspond to particles *2* in Fig. 3*d*. The same particles were implied when we spoke of the structure detected by scanning electron microscopy and presented in Fig. 6*b*.

The mean size of the finest particles precipitated from α-Fe is about 20 nm. Most particles of this kind are distributed uniformly inside the ferrite spaces of the pearlite (Fig. 7*b* and *c*). At the same time, the origin of some of the copper-containing particles is connected with manifestation of a heterophase nucleation mechanism. Transmission electron microscopy shows the presence of particles shaped as flattened drops on the surface of cementite plates of the pearlite (Fig. 7*c*). The diameter of the particles is 5 – 10 nm larger than the sizes of single fine particles in the ferrite. They have formed due to the same supersaturation of the ferrite matrix with copper under cooling of the alloy to room temperature. Analysis of the microdiffraction patterns shows that the mutual crystallographic orientation of the lattices of ε-Cu and α-Fe is close to the Kurdyumov–Sachs orientation relation, i.e., $(011)_{Cu} \parallel (111)_{\alpha\text{-Fe}}$, $[1-11]_{Cu} \parallel [01-1]_{\alpha\text{-Fe}}$.

A special feature of copper-alloyed cast irons is preferred precipitation of crystals of secondary cementite on interfaces of ε-Cu and the surrounding austenite (see Fig. 8). The data of the metallographic analysis show that the absolute majority of microvolumes of ε-Cu are covered partially or completely with a cementite shell. The typical plate shape of the crystals indicates the presence of Widmanstatten cementite near many particles of ε-Cu. It should be stressed that secondary cementite forms by diffusion of carbon from the austenite matrix to copper-containing inclusions in molten condition. The temperature range matching this process is bounded by points *c* and *d* in Fig. 1. The liquid condition of the copper-enriched microvolumes is proved by the shape of the interfaces of coarse ε-Cu particles and precipitates of secondary cementite (Fig. 8*b*). The structural studies have shown that the growing cementite crystals penetrate many particles of ε-Cu. It is obvious that in the process of rapid enough cooling of the ingot these significant transformations of the shape of the copper-containing particles having a solid-phase condition cannot occur, because the diffusion of copper in the austenite and cementite is very low. However, if the copper-containing phase is in a liquid condition, the cementite crystals growing toward it penetrate the melt easily and transform the shape of the interface.

The data of the x-ray diffraction analysis of the irons alloyed with copper and aluminum are presented in Fig. 9. Deciphering of the diffraction pattern of the iron with minimum

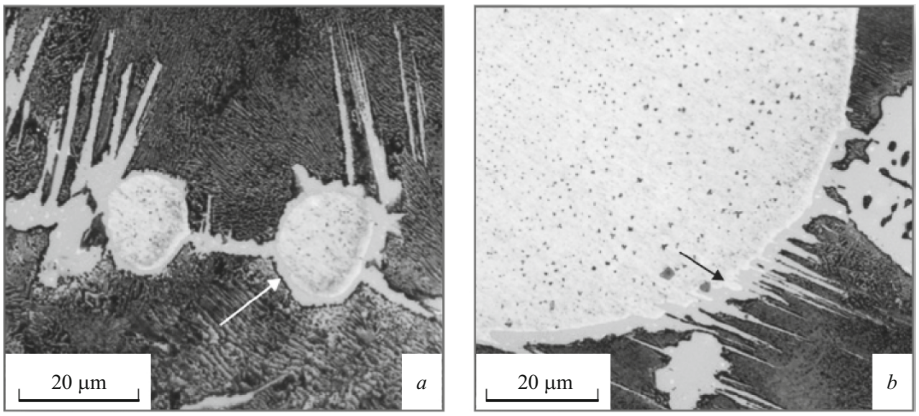

Fig. 8. Precipitation of secondary cementite on the boundaries of a junction of ε-Cu and pearlite particles in SCh14.7Cu (marked with the arrows).

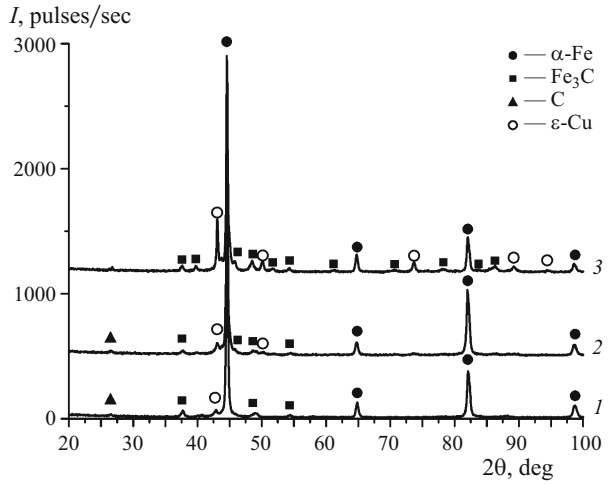

Fig. 9. Diffraction patterns for cast irons with different copper contents: *1*) 0.08% Cu; *2*) 6.57% Cu; *3*) 14.7% Cu.

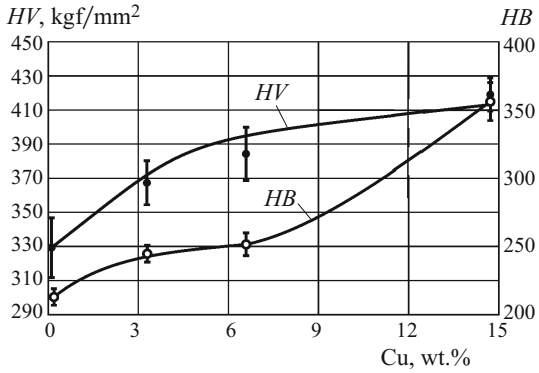

Fig. 10. Microhardness *HV* of pearlite and hardness *HB* of cast iron as a function of the copper content.

copper content (0.08% Cu) shows the presence of cementite, graphite, and a solid solution based on α-Fe with parameter 2.872 Å of the elementary cell. Growth of the copper content to 3.27% raises the parameter of the elementary cell of α-Fe to 2.876 Å, which follows from the shift of the peaks toward lower angles. Further growth of the copper content does not affect noticeably the parameter of the elementary cell of α-Fe. The increase in value of the parameter from 2.872 Å to 2.876 Å may be associated with dissolution of copper in the ferrite matrix of the iron. It should be stressed that most of the works devoted to the analysis of alloys of the Fe – Cu system mention virtually total insolubility of copper in iron at room temperature [17]. It is possible that the features of the solubility of copper in the α-Fe observed in the present work are explainable by the presence of 0.9% Al in the alloys. Increase of the copper content from 3.27% to 14.7% has not changed the parameter of the elementary cell of α-Fe. This means that copper does not dissolve additionally in the ferrite lattice. The first peaks corresponding to ε-Cu have been detected at 3.27% Cu in the alloy. The parameter of the elementary cell of this type of solid solution type is 3.607 Å. Growth of the copper content from 6.57% to 14.7% increases the parameter of the elementary cell to 3.624 and 3.637 Å, respectively.

When the copper content is varied within 0.08 – 14.7%, the microhardness of the plate pearlite in the cast irons increases from 330 to 415 *HV* (Fig. 10). The growth in the microhardness is the most noticeable in the range from 0.08 to 3.27% Cu. The causes of this phenomenon are refinement of the ferrite-cementite mixture and precipitation of nanosize particles of ε-Cu in the ferrite spaces. The copper-containing inclusions distributed uniformly in the ferrite are effective barriers for the moving dislocations. The growth of the microhardness of the pearlite due to the dissolution of copper in the ferrite matrix seems to be minimal. Similar data have been obtained in [21] in a study of the effect of copper on the microhardness of a low-carbon steel.

The growth of the microhardness of the pearlite is accompanied by elevation of the hardness of the metal, which follows from the results obtained with the use of the Brinell method. Introduction of 14.7% Cu into the alloy increases its hardness by 155 *HB* (from 200 to 355 *HB*) (Fig. 10). However, we should not associate the mentioned increase only with the hardening of the plate ferrite. Another factor explaining the change in the level of the hardness upon introduction of copper into cast iron is decrease in the content of

graphite and formation of ledeburite in the alloys. The hardening effect due to the formation of ledeburite is manifested the most in the case of 6.57% Cu in the alloy.

CONCLUSIONS

Analysis of the amended Fe – Cu – C phase diagram designed with the use of the FactSage software shows different origins of the copper-enriched ε-Cu particles, which results in differences in the sizes of the precipitates formed in the iron from the liquid melt, austenite and ferrite. The sizes of the ε-Cu inclusions formed in the iron with 14.7% Cu range from 5 nm to 250 μm, i.e., differ by more than 4.5 orders of magnitude. The average size of the ε-Cu particles appearing upon stratification of the melt into a two-phase liquid amounts to 20 – 30 μm. The particles of ε-copper precipitated over the boundaries of the austenite grains have a size of 1 – 5 μm. The size of the ε-Cu particles formed inside the austenite grains amounts to about 200 nm. The finest particles with a mean size of about 20 nm precipitate from α-Fe and are distributed inside ferrite spaces in pearlite colonies. The result of the higher fineness of the ferrite-cementite mixture and of the formation of numerous nanosize particles of ε-Cu is growth in the microhardness of the colonies of plate pearlite from 330 to 415 *HV*.

The work has been performed within a grant of the Russian Scientific Foundation (Project No. 15-19-00230).

REFERENCES

1. G. I. Sil'man, V. V. Kamynin, and V. V. Goncharov, "On the mechanism of copper effect on formation of structure in cast iron," *Metalloved. Term. Obrab. Met.*, No. 9, 16 – 22 (2007).
2. E. D. Golovin, V. A. Kuznetsov, V. Kumar, et al., "Effect of copper on the antifriction properties of gray cast irons," *Obrab. Met. Tekhnol. Oborud. Instr.*, No. 1(54), 81 – 84 (2012).
3. N. P. Lyakishev, *Phase Diagrams of Metallic Systems* [in Russian], Mashinostroenie, Moscow (1996), Vol. 2, 1024 p.
4. I. LeMay and L. M. D. Shettkey (eds.), *Copper in Ferrous Metals* [Russian translation] (1988), 311 p.
5. C. Chi, H. Yub, J. Dong, et al., "The precipitation strengthening behavior of Cu-rich phase in Nb contained advanced Fe – Cr – Ni type austenitic heat resistant steel for USC power plant application," *Progr. Nat. Sci. Mater. Int.*, **22**(3), 175 – 185 (2012).
6. F. A. Khalid and D. V. Edmonds, "On the properties and structure of micro-alloyed and copper-bearing hot-rolled steels," *J. Mater. Proc. Technol.*, **72**(3), 434 – 436 (1997).
7. L. Cao, S. Wu, and B. Liu, "On the Cu precipitation behavior in thermo-mechanically embrittlement processed low copper reactor pressure vessel model steel," *Mater. Design*, **47**, 551 – 556 (2013).
8. V. G. Gavriljuk, B. D. Shanina, and H. Berns, "On the correlation between electron structure and short range atomic order in iron-based alloys," *Acta Mater.*, **48**(15), 3879 – 3893 (2000).
9. X. Sauvage, N. Guelton, and D. Blavette, "Microstructure evolutions during drawing of a pearlitic steel containing 0.7 at.% copper," *Scr. Mater.*, **46**(6), 459 – 464 (2002).
10. G. Fourlaris, A. J. Baker, and G. D. Papadimitriou, "A microscopic examination of the precipitation phenomena occurring during the isothermal pearlitic transformation in high carbon-copper-nickel steels," *Acta Metall. Mater.*, **43**(12), 4421 – 4438 (1995).
11. G. Fourlaris, A. J. Baker, and G. D. Papadimitriou, "Microscopic characterisation of ε-Cu interphase precipitation in hypereutectoid Fe – C – Cu alloys," *Acta Metall. Mater.*, **43**(7), 2589 – 2604 (1995).
12. T. Chairuangsri and D. V. Edmonds, "The precipitation of copper in abnormal ferrite and pearlite in hyper-eutectoid steels," *Acta Mater.*, **48**(15), 3931 – 3949 (2000).
13. T. Chairuangsri and D. V. Edmonds, "Abnormal ferrite in hypereutectoid steels," *Acta Mater.*, **48**(7), 1582 – 1591 (2000),
14. E. Meslin, M. Lambrecht, M. Hernandez-Mayoral, et al., "Characterization of neutron-irradiated ferritic model alloys and a RPV steel from combined APT, SANS, TEM and PAS analyses," *J. Nucl. Mater.*, **406**(1), 73 – 83 (2010).
15. F. Hori, A. Morita, and R. Oshima, "Radiation-enhanced precipitation in FeCu(C) alloys studied by electron microscopy," *J. Electr. Miscrosc.*, **48**(5), 585 – 589 (1999).
16. Yu. G. Bobrov and L. A. Platonova, "Some features of the microstructure of aluminum irons alloyed with copper," in: *Advances in Cast Iron Metallography* [in Russian], Kiev (1981), pp. 94 – 99.
17. G. I. Sil'man, "About retrograde solidus and stratification of melt in the Fe – Cu and Fe – Cu – C systems," *Metal Sci. Heat Treat.*, **51**(1 – 2), 19 – 24 (2009).
18. K. Subhank and Y.-B. Kang, "Critical evaluation and thermodynamic optimization of Fe – Cu, Cu – C and Fe – C binary systems and Fe – Cu – C ternary system," *Calphad*, **45**, 127 – 137 (2014).
19. V. Raghavan, "C – Cu – Fe (carbon-copper-iron)," *J. Phase Equil. Diffus*., **33**(3), 224 – 225 (2012).
20. A. Yu. Yakovlev and I. P. Volchok, "Effect of copper on the structure and properties of graphitized copper," *Metalloved. Term. Obrab. Met.*, No. 1, 44 – 46 (2008).
21. E. Meslin, M. Lambrecht, M. Hernandez-Mayoral, et al., "Characterization of neutron-irradiated ferritic model alloys and a RPV steel from combined APT, SANS, TEM and PAS analyses," *J. Nucl. Mater.*, **406**(1), 73 – 83 (2010).